HHS Public Access

Author manuscript

Neurobiol Dis. Author manuscript; available in PMC 2018 December 01.

Published in final edited form as:

Neurobiol Dis. 2017 December ; 108: 183–194. doi:10.1016/j.nbd.2017.08.018.

Pro-excitatory alterations in sodium channel activity facilitate subiculum neuron hyperexcitability in temporal lobe epilepsy

Bryan S. Barker[1,2], **Aradhya Nigam**[1], **Matteo Ottolini**[1], **Ronald P. Gaykema**[1], **Nicholas J. Hargus**[1,2], and **Manoj K. Patel**[1,2]

[1]Department of Anesthesiology, University of Virginia Health System, Charlottesville, VA 22908 USA

[2]Neuroscience Graduate Program, University of Virginia Health System, Charlottesville, VA 22908 USA

Abstract

Temporal lobe epilepsy (TLE) is a common form of adult epilepsy involving the limbic structures of the temporal lobe. Subiculum neurons act to provide a major output from the hippocampus and consist of a large population of endogenously bursting excitatory neurons. In TLE, subiculum neurons are largely spared, become hyperexcitable and show spontaneous epileptiform activity. The basis for this hyperexcitability is unclear, but is likely to involve alterations in the expression levels and function of various ion channels. In this study, we sought to determine the importance of sodium channel currents in facilitating neuronal hyperexcitability of subiculum neurons in the continuous hippocampal stimulation (CHS) rat model of TLE. Subiculum neurons from TLE rats were hyperexcitable, firing a higher frequency of action potentials after somatic current injection and action potential (AP) bursts after synaptic stimulation. Voltage clamp recordings revealed increases in resurgent (I_{NaR}) and persistent (I_{NaP}) sodium channel currents and pro-excitatory shifts in sodium channel activation and inactivation parameters that would facilitate increases in AP generation. Attenuation of I_{NaR} and I_{NaP} currents with 4,9-anhydro-tetrodotoxin (4,9-ah TTX; 100 nM), a toxin with increased potency against $Na_v1.6$ channels, suppressed neuronal firing frequency and inhibited AP bursting induced by synaptic stimulation in TLE neurons. These findings support an important role of sodium channels, particularly $Na_v1.6$, in facilitating subiculum neuron hyperexcitability in TLE and provide further support for the importance of I_{NaR} and I_{NaP} currents in establishing epileptiform activity of subiculum neurons.

Keywords

Subiculum; Temporal lobe epilepsy; Action potentials; Sodium channels; Electrophysiology; $Na_v1.6$

Corresponding author: Manoj K. Patel, Ph.D., Department of Anesthesiology, University of Virginia Health System, Charlottesville VA, 22908-0710, USA. Tel: +1 434 924 9693 Fax: +1 434 924 2105, mkp5u@virginia.edu.

Introduction

Temporal lobe epilepsy (TLE) is a common type of adult epilepsy and is characterized by the occurrence of spontaneous, recurrent seizures that originate from limbic structures of the temporal lobe (Spencer and Spencer, 1994). Seizures associated with TLE can be difficult to treat with up to 30% of patients being considered therapy resistant (Kwan and Sander, 2004). While the hippocampus proper and the entorhinal cortex have been extensively examined in TLE (Buckmaster and Dudek, 1997; Hargus et al., 2013; Hargus et al., 2011; Sanabria et al., 2001), the subiculum remains largely understudied in the disease. The subiculum receives input from the CA1 and entorhinal cortex layer II/III. In turn, the subiculum provides excitatory input to CA1, deep layers of the entorhinal cortex and other subcortical and cortical regions (O'Mara et al., 2001; Shao and Dudek, 2005; Swanson and Cowan, 1977; Witter and Groenewegen, 1990). In addition to propagating information out the hippocampus proper, the subiculum can also prevent neuronal signaling from spreading and acting as a gate, via $GABA_A$ receptor signaling, to control hippocampal and parahippocampal interactions. This characteristic has even been shown to shunt epileptiform activity, preventing it from spreading to the entorhinal cortex in *in vitro* models of TLE (Benini and Avoli, 2005). A large population of subiculum neurons are endogenously bursting (Staff et al., 2000). This bursting characteristic, along with the many reciprocating inputs between the subiculum, the hippocampus proper and the entorhinal cortex have implicated the subiculum in not only amplifying synaptic information received, but to also provide loop circuits within the hippocampal/entorhinal cortex network, facilitating neuronal synchronization (Harris and Stewart, 2001; Naber et al., 2001).

Several lines of evidence support a role for the subiculum in initiating seizure generation in both human patients and animal models of TLE. Firstly, subiculum neurons are spared in patients with TLE and may even increase in density (Alonso-Nanclares et al., 2011; Dawodu and Thom, 2005; Fisher et al., 1998), unlike hippocampal neurons where significant neuronal loss occurs (Bernasconi, 2003; Houser, 1990; Mathern et al., 1995). Recordings from resected brain tissue obtained from patients with refractory TLE revealed synchronous spontaneous inter-ictal like epileptiform bursts within the subiculum, but not the hippocampus (Cohen et al., 2002; Wozny et al., 2005). Studies using animal models of TLE support the human patient observations, demonstrating early preictal increases in action potential (AP) firing of subiculum excitatory and inhibitory neurons (Fujita et al., 2014; Toyoda et al., 2013). An increase in the number of bursting subiculum neurons along with augmented post-burst after depolarizations has also been reported in TLE, (Wellmer et al., 2002), although this may be region specific (Knopp et al., 2005). Increased sprouting from surviving CA1 neurons onto subiculum neurons could lead to a further enhancement of synchronized epileptiform activity (Cavazos et al., 2004; de Guzman et al., 2006).

In addition to alterations in synaptic connectivity, intrinsic alterations are also likely to occur in TLE, driving neuronal network hyperexcitability. Alterations in voltage gated sodium channel physiology have been implicated in facilitating and maintaining increases in neuronal excitability in epilepsy (Agrawal et al., 2003; Aronica et al., 2001; Hargus et al., 2013; Hargus et al., 2011; Ketelaars et al., 2001; Vreugdenhil et al., 2004; Whitaker et al., 2001) and subiculum neurons isolated from patients with intractable TLE exhibit increased

persistent sodium currents (Vreugdenhil et al., 2004). The sodium channel isoform, $Na_v1.6$, has received much attention in the development of neuronal hyperexcitability since it is highly expressed along the axon initial segment (AIS) (Hu et al., 2009) where it plays a significant role in the initiation of APs (Royeck et al., 2008) and also along nodes of Ranvier, facilitating saltatory conduction (Boiko et al., 2001; Kaplan et al., 2001). Increases in $Na_v1.6$ activity have been implicated in facilitating neuronal hyperexcitability in entorhinal cortex neurons (Hargus et al., 2013; Hargus et al., 2011) and is increased in kindled animals (Blumenfeld et al., 2009). Moreover, reducing $Na_v1.6$ levels impairs the initiation and development of kindled seizures (Blumenfeld et al., 2009), inhibits spontaneous firing and chemically induced seizures, and reduces firing frequencies in various neurons (Makinson et al., 2014; Raman and Bean, 1997; Royeck et al., 2008; Van Wart and Matthews, 2006). Furthermore, gain-of-function mutations of $Na_v1.6$ lead to pro-excitatory alterations in channel function (Barker et al., 2016) and spontaneous seizures in human patients and in a knock-in mouse model (Veeramah et al., 2012; Wagnon et al., 2015).

The importance of sodium channels in facilitating increases in subiculum neuron excitability in epilepsy has yet to be determined. In the current study we investigated if sodium channel function was altered in subiculum neurons in TLE using the continuous hippocampal stimulation (CHS) rat model. Additionally, we wanted to see if persistent (I_{NaP}) and resurgent (I_{NaR}) sodium channel currents were increased in TLE. I_{NaP} currents are slow inactivating currents that arise in subthreshold voltage ranges and are capable of amplifying a neuron's response to synaptic input (Stafstrom, 2007). I_{NaR} currents occur from channel re-opening during the repolarization phase of the AP and both I_{NaR} and I_{NaP} have been shown to facilitate bursting APs and high frequency AP firing (Lewis and Raman, 2014; Raman and Bean, 1997; Stafstrom, 2007; van Drongelen et al., 2006; Yue et al., 2005) Here we show that bursting subiculum TLE neurons are hyperexcitable and display increased persistent (I_{NaP}) and resurgent (I_{NaR}) sodium currents. Pro-excitatory alterations in sodium channel activation and inactivation gating were also detected. Using a tetrodotoxin metabolite, 4,9-anhydro-TTX to inhibit mainly $Na_v1.6$ channels (Rosker et al., 2007), we show that inhibition of I_{NaP} and I_{NaR} currents leads to attenuation of subiculum neuronal hyperexcitability and burst firing associated with TLE. We propose that increases in I_{NaP} and I_{NaR} currents and pro-excitatory changes in sodium channel physiology, together with synaptic network changes, contribute to the hyperexcitability of subiculum neurons in TLE, which aid in seizure initiation and seizure spread throughout the temporal lobe.

Materials and Methods

Animals

All animal experiments were conducted in accordance with the guidelines established by the National Institutes of Health guide for the Care and Use of Laboratory Animals and were approved by the University of Virginia's Institute of Animal Care and Use Committee. Adult male Sprague–Dawley rats (250–300 grams) received a bipolar twisted pair of stainless steel electrodes to either hemisphere unilaterally in the posterior ventral hippocampus for stimulation and recording (coordinates from bregma AP~−5.3 mm, ML~4.9 mm, DV~5.0

mm, bite at ~−3.5 mm) (Paxinos and Watson, 2006). Electrodes were attached to Amphenol connectors and secured to the skull with jeweler's screws and dental acrylic. One week following surgery, rats were stimulated through the hippocampal electrode to induce limbic *status epilepticus* using a protocol previously described (Lothman et al., 1989). In brief, animals were stimulated for 90 min with 10-s trains of 50 Hz, 1 ms biphasic square waves with a maximum intensity of 400 μA peak to peak delivered every 11 s. Following the induction of and recovery from limbic *status epilepticus*, rats were placed in standard laboratory housing. Three months after the induction of *status epilepticus*, animals were evaluated for the presence and frequency of spontaneous temporal lobe seizures (Bertram and Cornett, 1994). During the monitoring phase, rats were placed in specially designed cages, which allowed full mobility of the animals, good visualization for video monitoring, and a stable recording environment. Animals had free access to food and water, as well as a standard 12 h light–dark cycle. Seizures were recorded and documented using a commercial computerized EEG program (Harmonie, Stellate Systems). All data were reviewed at an offline reading station connected to the vivarium computers via a local area network. The time of occurrence, behavioral severity (Racine 5 point scale) and duration for all seizures were noted.

Seizure determination

Electrographic seizures in the rats were characterized by the paroxysmal onset of high frequency (greater than 5 Hz) increased amplitude discharges that showed an evolutionary pattern of a gradual slowing of the discharge frequency and subsequent post-ictal suppression. Seizure duration was measured from the onset of the high frequency activity or initial spike to the cessation of the terminal regular electrographic clonic activity.

Brain Slice Preparation and Action Potential Recordings

Horizontal brain slices (300 μm) were prepared from adult male Sprague–Dawley rats (350–450 grams). Rats were euthanized with isoflurane, decapitated, and brains rapidly removed and placed in chilled (4°C) artificial cerebrospinal fluid (ACSF) containing (in mM): 125 NaCl, 2.5 KCl, 1.25 NaH_2PO_4, 2 $CaCl_2$, 1 $MgCl_2$, 0.5 L-Ascorbic acid, 10 glucose, 25 $NaHCO_3$, and 2 Pyruvate (oxygenated with 95% O_2 and 5 % CO_2, osmolarity adjusted to 310 mosM with sucrose). Slices were prepared using a Vibratome (Vibratome 1000 Plus), transferred to a chamber containing oxygenated ACSF, incubated at 37°C for 45 minutes, and then stored at room temperature. For recordings, slices were held in a small chamber and superfused with heated (32°C) oxygenated ACSF. Subiculum bursting neurons were found to be in high density in the distal pyramidal layer just adjacent to the presubiculum. The subiculum pyramidal layer was identified by infra-red video microscopy (Hamamatsu, Shizouka, Japan) using a Zeiss Axioscope microscope. Whole-cell voltage and current clamp recordings were performed using an Axopatch 700B amplifier (pCLAMP 10 software, Molecular Devices) and a Digidata 1322A (Molecular Devices). Electrodes were fabricated from borosilicate glass using a Brown-Flaming puller (model P97, Sutter Instruments Co) and had resistances of 3.5–4.0 MΩ when filled with an intracellular recording solution containing (in mM): 120 potassium-gluconate, 10 NaCl, 2 $MgCl_2$, 0.5 K_2EGTA, 10 HEPES, 4 Na_2ATP, 0.3 NaGTP (pH adjusted to 7.2 with KOH, osmolarity adjusted to 300 mosM with sucrose). Currents were amplified, low-pass filtered (2 kHz), and

sampled at 33 kHz. APs were evoked with a series of current injection steps from −20 pA to 470 pA in 10 pA steps for 300 ms at 5 sec inter-pulse intervals. To standardize our tests the resting membrane potential (RMP) was recorded and then maintained at −65 mV by injection of DC current. Cell input resistance (IR) was calculated by dividing the steady-state voltage response evoked by varying current injections (ΔV/ΔI) from −20 pA until the current pulse just prior to that which evoked an AP. Data points were then fit with a linear line to determine IR values. Threshold was determined as the voltage at which the slope of the AP exceeded ≥ 20 Vs^{-1}. AP amplitudes were measured from threshold to the AP peak. Width was the duration of the AP at the half way voltage between threshold and AP peak. Upstroke velocity was determined from phase plots using the maximum of the first derivative (dV/dt). In some experiments APs were evoked using a bipolar platinum iridium stimulating electrode (WPI, Sarasota, FL, USA) placed in the pyramidal layer CA1 approximately 5 cm proximal to the subiculum-CA1 border. A 400 μs stimulus of varying current amplitude (1 to 3.2 mA) was applied every 15 sec via a digital stimulator (Digitimer Ltd, Hertfordshire, UK). In order to consistently evoke APs the stimulus amplitude was increased 1.5 times from threshold.

Sodium Channel Electrophysiology

All sodium channel current recordings, except for persistent sodium currents (I_{NaP}) and resurgent sodium currents (I_{NaR}), were recorded using the outside-out recording configuration of the patch clamp recording technique. Currents were amplified, low-pass filtered (2 kHz), and sampled at 33 kHz. Glass pipettes had resistance of 1.8 – 2.5 mΩ when filled with the following electrode solution (in mM): 140 CsF, 2 $MgCl_2$, 1 EGTA, 10 HEPES, 4 Na_2ATP, and 0.3 NaGTP (pH adjusted to 7.3 with CsOH, osmolarity adjusted to 310 mosM with sucrose). Outside-out patches were superfused with solution containing the following composition (in mM): 150 NaCl, 2.5 KCl, 2 $CaCl_2$, 1 $MgCl_2$, 1.25 NaH_2PO_4, 0.5 L-Ascorbic acid, 2 Pyruvate, 10 Glucose, 25 $NaHCO_3$ (pH adjusted by bubbling CO_2/O_2, osmolarity adjusted to 320 mosM with sucrose). All experiments were performed at 32 °C. Capacitive and leak currents were subtracted using the P/N-4 protocol. The current-voltage relationship was determined using a 100 ms voltage pulse from −80 to +5 mV in steps of 5 mV from a holding potential of −120 mV at 2 sec intervals. Conductance as a function of voltage was derived from the current-voltage relationship and fitted by a Boltzmann function as previously described (Hargus et al., 2011)

For steady-state inactivation, neurons were held at −120 mV and test potentials from −115 mV to −25 mV for 500 ms at 5 mV increments were applied. The second pulse to −10 mV for 40 ms was used to assess channel availability. Currents during the second pulse were normalized for each cell with the largest current as 1.0 and fit to the Boltzmann function.

Persistent sodium currents (I_{NaP}) were determined in brain slice preparations using voltage ramps from −100 mV to −10 mV at a rate of 65 mV/s. I_{NaP} was recorded in bath solution containing (in mM): 30 NaCl, 120 TEA-Cl, 10 $NaHCO_3$, 1.6 $CaCl_2$, 2 $MgCl_2$, 0.2 $CdCl_2$, and 5 4-AP, 15 Glucose (pH 7.4 when oxygenated with 95% O_2 and 5% CO_2; temperature 32°C, osmolarity adjusted to 310 mosM with sucrose) and a pipette solution containing (in mM): 140 CsF, 2 $MgCl_2$, 1 EGTA, 10 HEPES, 4 Na_2ATP, and 0.3 NaGTP (pH adjusted to

7.3 with CsOH, osmolarity adjusted to 300 mosM with sucrose). Ramp voltage recordings displayed an inward current that was referred to as I_{NaP}. To determine the peak I_{NaP} current, voltage ramp protocols were repeated in the presence of tetrodotoxin (TTX; 1 μM). Traces obtained in the presence of TTX were subtracted from those obtained in its absence. TTX was reconstituted in ACSF.

Resurgent sodium currents (I_{NaR}) were also recorded in brain slice preparation using a bath solution containing (in mM): 100 NaCl, 26 $NaHCO_3$, 19.5 TEA-Cl, 3 KCl, 2 $MgCl_2$, 2 $CaCl_2$, 2 $BaCl_2$, 0.1 $CdCl_2$, 4 4-AP, and 10 glucose (pH 7.4 when oxygenated with 95% O_2 and 5% CO_2; osmolarity adjusted to 310 mosM with sucrose; temperature 32°C) using the same pipette solution as that for recording I_{NaP}. Neurons were held at −100 mV and depolarized to +20 mV for 20 ms, followed by either a single repolarizing step to −30 mV for 100 ms to determine the peak I_{NaR}, or by using a series of repolarizing steps from −100 mV to −10 mV to determine the voltage dependence of I_{NaR}. Protocols were again repeated in the presence of TTX (1 μM) to determine I_{NaR} current amplitudes and gating.

Immunohistochemistry

TLE and aged matched WT rats (4 rats for each group, 350–450 grams) were euthanized with isoflurane, decapitated, and brains rapidly removed and placed in chilled (4°C) ACSF. Horizontal 500 μm thick sections were prepared using a Vibratome, and transferred to a chamber containing oxygenated ACSF at 37°C and incubated for 35 minutes. Slices were then embedded in OCT Compound in cryomolds and snap-frozen on dry ice-chilled isopentane, and kept on dry ice. Cryostat sections (16 μm) were prepared and thaw-mounted onto Superfrost Plus slides (Fisher Scientific) and stored at −80 °C for no more than 3 days prior to further processing. Slices were fixed in ice-cold acetone-ethanol mixture for 5 min, air-dried, washed with KPBS and then placed for 60 min in KPBS blocking solution (5% fish skin gelatin, 5% normal goat serum, 0.25% Triton X 100, and 0.65% w/v BSA), followed by incubation in blocking solution containing the pair of primary antibodies for 48 h at 4 °C (rabbit anti-$Na_v1.6$, 1:500, Alomone labs), and monoclonal mouse anti-Ankyrin G (1:500, NeuroMab). The slides were then washed with KPBS, incubated in blocking solution containing a pair of secondary antibodies (Alexa 488-conjugated goat anti-mouse IgG and Alexa 555-conjugated goat anti-rabbit IgG, both at 1:1000, Thermo Fisher Scientific). Slides were washed in KPBS, incubated in Nuclear Blue (1 drop/ml, Invitrogen), washed, air-dried, and cover slipped in Polymount (Polysciences Inc.).

Confocal images were captured of subiculum neurons using a Zeiss LSM 710 confocal microscope (Zeiss, Oberkochen, Germany) with a 63x oil immersion objective and ZEN Zeiss LSM Imaging software. The settings of the laser intensities and image capture were initially optimized but then not changed during the scanning of the slides. Quantification and analysis was performed using Image J software. For analysis of $Na_v1.6$ expression, a line scan representing the length of the AIS, as determined by Ankyrin G staining, was drawn, and the mean relative optical density (R.O.D) determined. The mean R.O.D for Ankyrin G was unaltered between WT and TLE preparations and allowed for standardization of the immunolabeling as a ratio of $Na_v1.6$ to Ankyrin G staining for each AIS.

Data Analysis

Electrophysiology data analysis was performed using Clampfit software (v10, Molecular Devices) and Matlab (Mathworks). Data represent means ± standard error of the mean (SEM). Statistical significance was determined using a Student's t-test with Welch's Correction. (GraphPad Prism 6).

Results

Subiculum bursting neurons are hyperexcitable in TLE

Subiculum bursting neurons were found to be in high density in the distal pyramidal layer just adjacent to the presubiculum, and WT neurons were distinguished by their propensity to produce a burst of APs at the onset of depolarization, followed by more tonic spiking (Figure 1A; WT) (Mattia et al., 1993; Petersen et al., 2017; Staff et al., 2000; Stewart and Wong, 1993; Taube, 1993). In contrast, subiculum neurons from TLE animals were hyperexcitable, firing more than a single burst of APs at lower current injection steps compared to WT (Figure 1A; TLE). Over a series of depolarizing current injection steps (50 pA to 470 pA) TLE neurons fired a significantly greater number of APs than WT ($P<0.05$, Figure 1A–B). We measured the maximal negative repolarizing voltage between APs for those evoked by a current injection step of 270 pA (Figure 1C). In TLE subiculum neurons the maximal negative voltage attained after the completion of repolarization was significantly depolarized compared with WT neurons ($P<0.01$ for APs 1, 3 and 4 and $P<0.05$ for APs 2 and 5; Figure 1C). These data indicate the presence of an increased sustained depolarizing current in TLE neurons that would drive neurons to spiking thresholds, accounting for the earlier AP initiation in TLE neurons. Analysis of AP properties revealed a significantly hyperpolarized threshold, a significant increase in input resistance (IR) and AP width in TLE neurons compared to WT. No significant differences were seen in resting membrane potential (RMP), AP amplitude or AP upstroke velocity (Table 1).

Brief stimulation of the pyramidal layer of CA1 consistently evoked AP bursts in both control and TLE subiculum neurons (Figure 1D & E). In TLE neurons, the average number of APs evoked was 3.2 ± 0.1 (n=8). In contrast, WT neurons were less excitable and evoked 2.1 ± 0.1 APs, (n= 8; $P<0.01$). Synaptically evoked bursts in TLE neurons were also longer lasting than those recorded in WT neurons (Figure 1D & F). To better quantify this increase in burst duration, we measured the area under the curve (AUC) for AP trains evoked by synaptic stimulation in both WT and TLE subiculum neurons. Compared to WT neurons, TLE neurons showed a significant increase in AUC ($P<0.01$; Figure 1F) further suggesting the presence of a greater depolarizing current in TLE neurons.

Pro-excitatory shifts in sodium channel activation and inactivation gating in subiculum TLE neurons

To explore if pro-excitatory alterations in sodium channel physiology play a significant role in increased subiculum hyperexcitability in TLE, sodium channel currents were recorded using outside-out patches from visually identified subiculum pyramidal neurons in brain slice preparations. Representative macroscopic sodium currents from WT and TLE subiculum neurons are shown in Figure 2A. Sodium channel current densities from outside-

out recordings were not significantly different between genotypes (Data not shown). Analysis of current-voltage (I–V) curves revealed a significant 6.3 mV hyperpolarizing shift in the $V_{1/2}$ of activation in TLE neurons (n=14) compared to WT (n=19, P<0.05; Figure 2B & C; Table 2). Slope factor (k) was also increased in TLE subiculum neurons compared with WT (P<0.05, Figure 2D, Table 2). In addition to alterations in activation parameters, inactivation parameters were also altered in TLE neurons with a 5.7 mV depolarizing shift in the $V_{1/2}$ (n=18) compared to WT neurons (n=12, P<0.05; Figure 2E & F, Table 2). Slope factor (k) was not changed (Figure 2G, Table 2). Window currents were estimated from the area under the overlapping normalized activation and inactivation curves. Predicted window currents for TLE subiculum neurons were increased 2.6-fold and were persistent over a greater voltage range than WT cells (Figure 2H).

Subiculum bursting TLE neurons have increased persistent (I_{NaP}) and resurgent (I_{NaR}) currents

Persistent sodium currents (I_{NaP}) are thought to be a major contributor to the generation of AP bursts and have been recorded from a portion of isolated subiculum neurons from TLE patients (Vreugdenhil et al., 2004). I_{NaP} currents were recorded using slow voltage ramps using brain slice preparations. Ramp recordings displayed a robust inward current that was abolished by application of 1μM TTX. The peak I_{NaP} was calculated by subtracting traces obtained in the presence of TTX from those obtained in the absence of the toxin. In TLE subiculum neurons, we observed a significant increase in I_{NaP} currents compared to WT cells (Figure 3A–C). I_{NaP} currents from WT subiculum neurons had a peak amplitude of −160 ± 35 pA (n= 7). In contrast, peak I_{NaP} currents from TLE neurons were increased 7.5 fold to −1206 ± 104 pA (n= 6, P<0.01; Figure 3A–C). No significant differences were seen in the voltage-dependence or time course of activation of I_{NaP} (data not shown).

Resurgent sodium currents (I_{NaR}) are depolarizing currents that play a significant role in enhancing firing frequency or bursting activity (Raman and Bean, 1997). It is believed that I_{NaR} occurs from channel re-opening during the repolarization phase of the AP that arises from the electrostatic repulsion of an open-channel blocker (Lewis and Raman, 2014; Patel et al., 2016). Peak I_{NaR} currents were elevated by 92% in TLE subiculum neurons (−1208 ± 122 pA, n= 6) compared with WT (−629 ± 62 pA, n= 9, P<0.01; Figure 3D–F). Similar to I_{NaP}, no significant differences were seen in the voltage-dependence or time course of activation of I_{NaR} (data not shown).

The $Na_v1.6$ isoform is considered to be one of the most significant contributors to both I_{NaR} and I_{NaP} (Hargus et al., 2013; Raman and Bean, 1997). The observed increase in both I_{NaR} and I_{NaP} in TLE subiculum bursting neurons could be accounted for by pro-excitatory alteration in $Na_v1.6$ physiology function that could facilitate neuronal hyperexcitability. To test this hypothesis, we used the TTX metabolite 4,9 anhydro-tetrodotoxin (4,9-ah-TTX), which has a greater affinity for $Na_v1.6$ over other sodium channel isoforms, making the toxin a valuable tool for studying $Na_v1.6$ in neuronal physiology (Hargus et al., 2013; Rosker et al., 2007). Previous studies have shown that at a concentration of 100 nM, 4,9-ah-TTX inhibits approximately 50% of $Na_v1.6$ channels stably expressed in HEK 293 cells without any effect on $Na_v1.2$ channels (Hargus et al., 2013). We tested the effects of 100 nM

4,9-ah-TTX on both I_{NaR} and I_{NaP} currents. 4,9-ah-TTX (100 nM) significantly reduced I_{NaP} in TLE subiculum neurons by 64.5% (from −1206 ± 104 pA, n=6 to −428 ± 74 pA, n=6, P<0.01; Figure 3B & C). In WT subiculum neurons, 4,9-ah-TTX (100 nM) caused a small decrease in I_{NaP}, by 37.5% (from 160 ± 35 pA, n= 7 to −100 ± 25 pA, n=7, Figure 3A & C). 4,9-ah-TTX had no effect on I_{NaP} activation parameters (data not shown).

In a similar manner to effects observed with I_{NaP} currents, 4,9-ah-TTX (100 nM) also reduced I_{NaR} currents in TLE subiculum neurons by 48.5% (from −1208 ± 122 pA, n= 6 to −622 ± 103 pA, n=6, P<0.01; Figure 3E & F). I_{NaR} currents were also reduced in WT neurons by 4,9-ah-TTX (100 nM; from −629 ± 62.6 pA, n= 9 to −344.5 ± 34.4 pA, n=9, P<0.05; Figure 3D & F). Once again, 4,9-ah-TTX had no effects on I_{NaR} activation parameters (data not shown).

Inhibition of $Na_v1.6$ suppresses neuronal excitability

Both I_{NaR} and I_{NaP} currents are important for controlling neuronal excitability and reductions in I_{NaR} and I_{NaP} currents by 4,9-ah-TTX should modulate neuronal excitability. To test this hypothesis we determined the effects of 4,9-ah-TTX (100 nM) on APs evoked by both somatic current injection and by synaptic stimulation. 4,9-ah-TTX (100 nM) significantly reduced AP frequency in both WT and TLE subiculum bursting neurons (Figure 4A,C & E). At a current injection step of 470 pA, 4,9-ah-TTX (100 nM) decreased AP frequency in TLE neurons by 49.1% (from 44.4 ± 1.0 Hz, n=12 to 22.6 ± 1.0 Hz, n=6, P< 0.05; Figure 4C & E). In WT subiculum neurons 4,9-ah-TTX (100 nM) decreased AP frequency by 37.4% (from 36.6 ± 1.3 Hz, n=16 to 22.9 ±1.2 Hz, n=8, p< 0.05; Figure 4A & E).

Morphology of the first AP elicited by a depolarizing current injection step was characterized by phase plots of dV/dt vs voltage in WT and TLE neurons before and after the administration of 4,9-ah-TTX (100 nM; Figure 4B & D; Table 1). In WT neurons, AP thresholds were depolarized in the presence of 4,9-ah-TTX. In TLE subiculum neurons, 4,9-ah-TTX (100 nM) also depolarized AP thresholds and reduced upstroke velocity. Measurement of the maximal negative repolarizing voltage between APs at a current injection of 270 pA revealed a decreasing trend in both WT and TLE neurons, most likely the effect of inhibiting I_{NaP} and I_{NaR} currents. In WT, 4,9-ah-TTX (100 nM) significantly hyperpolarized inter AP voltages for the 2^{nd} AP (P<0.05; Figure 4F). For TLE neurons, 4,9-ah-TTX (100 nM) significantly hyperpolarized inter AP voltages for the 1^{st} AP (P<0.05; Figure 4G).

We determined the role of $Na_v1.6$ on synaptically evoked APs (Figure 5). Application of 4,9-ah-TTX (100 nM) significantly reduced synaptically evoked firing in TLE subiculum neurons from 3.2 ± 0.1 to 1.3 ± 0.2 APs in the presence of the toxin (n=8, P<0.01; Figure 5C & E). In WT subiculum neurons, synaptically evoked APs were also reduced by 4,9-ah-TTX (100 nM), reducing firing from 2.1 ± 0.1 to 1.5 ± 0.3 APs after application of the toxin (n=7; Figure 5A & E). However, the reduction in spiking did not reach significance (P<0.06). In addition to decreasing AP number, 4,9-ah-TTX (100 nM) significantly reduced the area under the curve (AUC) for TLE subiculum neurons, but not for WT cells (Figure 5F).

$Na_v1.6$ staining levels are not increased in TLE subiculum neurons

Increased staining for $Na_v1.6$ has been observed in TLE mEC neurons, suggesting an increase in $Na_v1.6$ expression levels (Hargus et al., 2013). To determine if $Na_v1.6$ staining was increased in subiculum neurons immunofluorescence experiments were performed. Robust $Na_v1.6$ staining was observed at the AIS and was co-localized with Ankyrin G (Ank G) staining, a marker for the AIS (Figure 6). Surprisingly, we saw no differences in the staining pattern for $Na_v1.6$ between WT and TLE subiculum neurons along the AIS.

Discussion

In this study, we investigated the importance of sodium channels in facilitating subiculum neuron hyperexcitability in TLE, the hallmark of seizures. The principal findings of this study are that subiculum neurons from TLE rats are 1) hyperexcitable, firing bursts of APs 2) exhibit pro-excitatory shifts in sodium channel activation and inactivation gating parameters, leading to an increase in the estimated sodium channel window current, 3) have increased resurgent (I_{NaR}) and persistent (I_{NaP}) sodium currents, two currents known to facilitate AP bursts, 4) pharmacological reduction of $Na_v1.6$ reduces both I_{NaR} and I_{NaP} sodium channel currents and attenuates neuronal firing frequency and AP bursts after synaptic stimulation. These findings provide new knowledge regarding the importance of sodium channels, particularly $Na_v1.6$, as a mechanism, in part, for the increases in neuronal excitability observed in epileptic subiculum bursting neurons.

The dramatic increases in I_{NaR} and I_{NaP} currents were a striking feature of epileptic subiculum neurons. I_{NaP} currents are non-inactivating currents that play a significant role in establishing repetitive neuronal discharge behavior (Stafstrom, 2007; van Drongelen et al., 2006; Yue et al., 2005). In naïve animals, CA1 I_{NaP} currents generate the somatic AP after depolarization potential (ADP), which is critical for controlling the firing mode of a neuron intrinsically (Yue et al., 2005). Non-inactivating currents recorded after the rapid transient sodium current and labeled as I_{NaP} currents, have been recorded from subiculum neurons in patients with intractable TLE (Vreugdenhil et al., 2004). Increases in I_{NaP} currents would significantly impact AP frequencies, providing a persistent depolarizing current on which APs would be initiated. In addition, greater I_{NaP} currents would contribute to lower firing thresholds and increased AP widths reported in TLE neurons, all of which were modulated by 4,9-ah-TTX. Although input resistances was also increased in TLE neurons, contributing to increased excitability, it is unlikely that increases in I_{NaP} currents played a major role since the addition of 4,9-ah-TTX caused a small, but non-significant reduction in R_i (Crill, 1996), suggesting involvement of additional ion channels.

Resurgent sodium currents (I_{NaR}) are depolarizing currents thought to play a significant role in enhancing firing frequency or bursting activity (Raman and Bean, 1997). It is believed that I_{NaR} occurs from channel re-opening during the repolarization phase of the AP that arises from the electrostatic repulsion of an open-channel blocker (Lewis and Raman, 2014; Patel et al., 2016). Our studies revealed large increases in I_{NaR} currents in TLE neurons, which in combination with increased I_{NaP} currents, would facilitate AP bursting in epilepsy. Increases in these two current types may provide a common mechanism by which a sustained and continuous depolarization could be achieved, leading to AP initiation.

Reducing I_{NaP} and I_{NaR} currents with 4,9-ah-TTX suppressed neuronal excitability and hyperpolarized the inter AP repolarizing voltage potentials. Since 4,9-ah-TTX at a concentration of 100 nM inhibits approximately 50% of $Na_v1.6$ channels (Hargus et al., 2013), these findings suggest a role for $Na_v1.6$, and particularly I_{NaP} and I_{NaR} currents in generating AP bursts (Rush et al., 2005). I_{NaR} and I_{NaP} currents were also increased in medial entorhinal cortex neurons of TLE rats and likely accounted for the increased AP frequency and neuronal hyperexcitability observed in that study (Hargus et al., 2013). Furthermore, increases in I_{NaR} currents are also an important feature for missense gain-of-function mutations of $Na_v1.6$, known to be responsible for epileptic encephalopathy in patients (Patel et al., 2016), speculating a causative role for this unique current in epilepsy.

The $Na_v1.6$ isoform is believed to be the main contributor of I_{NaR} and I_{NaP} (Rush et al., 2005) and CA1 pyramidal neurons from $Scn8a^{med}$ mice show significant reductions in I_{NaR} and I_{NaP} currents (Royeck et al., 2008). In agreement with those studies, inhibiting both I_{NaP} and I_{NaR} currents with 4,9-ah-TTX suppressed neuronal firing frequency and AP bursting in subiculum neurons. 4,9-ah-TTX is a TTX metabolite and has been reported to exhibit a <200 fold greater selectivity against $Na_v1.6$ over other TTX-sensitive isoforms when tested on sodium channels expressed in *Xenopus* oocytes (Rosker et al., 2007). However, in mammalian expression systems 4,9-ah-TTX is less selective for $Na_v1.6$ (Hargus et al., 2013). Using a concentration of 4,9-ah-TTX that is likely to inhibit approximately 50% of $Na_v1.6$ channels (100 nM) we found that 4,9-ah-TTX suppressed neuronal excitability to a greater degree in TLE subiculum neurons than WT neurons. The reductions in firing rates in TLE neurons were accompanied by significant depolarization of the resting membrane potential and AP threshold, an increase in AP width, and a decrease in AP upstroke velocity.

Our studies revealed pro-excitatory alterations in TLE subiculum neuron sodium channel physiology. Hyperpolarizing shifts in activation gating were coupled with depolarizing shifts in inactivation gating extending the voltage range where channels would be available for activation and have a finite probability of opening. The current established over this range is commonly referred to as the window current and an enhancement in this range, or "window," would increase the probability of channel opening, resulting in a reduction in AP thresholds, facilitating AP firing and potentially initiating seizure generation and spread. Increases in window currents have been associated with increased persistent sodium current activity and epileptogenesis in animal models of TLE (Ellerkmann et al., 2003; Ketelaars et al., 2001). In agreement, the voltage range of I_{NaP} currents reported in this study is consistent with the voltage range for the estimated window current.

A surprising finding was a lack of difference in $Na_v1.6$ staining intensity along the AIS between WT and TLE subiculum neurons. Previous studies in mEC neurons detected increases in $Na_v1.6$ staining, initiating as early as 7 days post-*status epilepticus* and continuing after 3 months, a time point where animals are in the chronic stage of epilepsy (Hargus et al., 2013; Hargus et al., 2011). These differences between studies suggest heterogeneity between neurons in TLE. It is possible that post translational modifications of $Na_v1.6$ in subiculum TLE neurons accounts for the increases in I_{NaR} and I_{NaP} currents and also alterations in activation and inactivation gating parameters. Downregulated phosphorylation coupled with increased methylation resulted in a 3-fold increase in $Na_v1.2$

channel current in a kainic acid model of TLE (Baek et al., 2014). Sodium channels are modulated by auxiliary subunits β subunits that notonly modulate surface expression, but also channel gating (Patino and Isom, 2010). The β4 subunit specifically plays a significant role in the generation of I_{NaR} current (Grieco et al., 2005). Modifications in β4 subunit expression or activity could occur in TLE, affecting I_{NaR} current physiology.

The subiculum receives dual afferent inputs from the CA1 pyramidal neurons as well as projections from neurons in the entorhinal cortex layers II/III (Stafstrom, 2005; M. P. Witter et al., 2000; M.P. Witter et al., 2000b). Conversely, the subiculum projects to a wide array of cortical and subcortical structures including recurrent projections back into the trisynaptic circuit via synapses with the entorhinal cortex (O'Mara et al., 2001; Shao and Dudek, 2005; Swanson and Cowan, 1977; Tang et al., 2016; Witter and Groenewegen, 1990). With its role as the output of the hippocampus and the presence of a large population of endogenously bursting neurons, the subiculum is perfectly predisposed to play a significant role in initiating and propagating epileptiform activity in TLE hippocampal circuitry (Harris and Stewart, 2001; Staff et al., 2000). In a study examining seizure initiation in a rat pilocarpine model of TLE, the subiculum was commonly the site of seizure initiation, and the site where ictal activity dissipated (Toyoda et al., 2013). Epileptiform activity originating in the subiculum can propagate to the CA1, driving hyperexcitability in hippocampal circuitry (Harris and Stewart, 2001). In human TLE patients, spontaneous rhythmic APs and epileptiform field potentials often originated in the subiculum before propagating into the hippocampus proper. This epileptiform activity persisted even when the subiculum was isolated, further supporting an intrinsic capability of the structure (Cohen et al., 2002).

Conclusion

In human patients and animal models of TLE, subiculum neurons are spared and become hyper-excitable leading to increased excitability within key hippocampal circuitry. As the output of the hippocampus, a hyperexcitable subiculum has the potential to both initiate and propagate epileptiform activity out of the temporal lobe leading to generalized ictal activity. Our findings support a role for sodium channels in facilitating subiculum neuronal hyperexcitability in TLE. We show that pro-excitatory shifts in sodium channel activation and inactivation parameters, as well as increases in I_{NaR} and I_{NaP} currents are prevalent in epileptic subiculum neurons. We suggest an important role for $Na_v1.6$ in facilitating these pro-excitatory alterations. Future intervention strategies that selectively target the $Na_v1.6$ isoform may be advantageous over current anticonvulsant therapies for seizure suppression.

Acknowledgments

This work was supported by National Institutes of Health/National Institute for Neurological Disorders and Stroke grants (NINDS) R01NS075157 (MKP), University of Virginia's Wagner Fellowship (BSB), and American Epilepsy Society's Predoctoral Research Fellowship (BSB).

References

Agrawal N, Alonso A, Ragsdale DS. Increased Persistent Sodium Currents in Rat Entorhinal Cortex Layer V Neurons in a Post-Status Epilepticus Model of Temporal Lobe Epilepsy. Epilepsia. 2003; 44:1601–1604. [PubMed: 14636336]

Alonso-Nanclares L, Kastanauskaite A, Rodriguez J-R, Gonzalez-Soriano J, DeFelipe J. A Stereological Study of Synapse Number in the Epileptic Human Hippocampus. Front Neuroanat. 2011:5. [PubMed: 21369363]

Aronica E, Yankaya B, Troost D, van Vliet EA, Lopes da Silva FH, Gorter JA. Induction of neonatal sodium channel II and III alpha-isoform mRNAs in neurons and microglia after status epilepticus in the rat hippocampus. Eur J Neurosci. 2001; 13:1261–6. [PubMed: 11285025]

Baek JH, Rubinstein M, Scheuer T, Trimmer JS. Reciprocal changes in phosphorylation and methylation of mammalian brain sodium channels in response to seizures. J Biol Chem. 2014; 289:15363–73. [PubMed: 24737319]

Barker BS, Ottolini M, Wagnon JL, Hollander RM, Meisler MH, Patel MK. The SCN8A encephalopathy mutation p. Ile1327Val displays elevated sensitivity to the anticonvulsant phenytoin. Epilepsia. 2016; 57:1458–1466. [PubMed: 27375106]

Benini R, Avoli M. Rat subicular networks gate hippocampal output activity in an in vitro model of limbic seizures. J Physiol. 2005; 566:885–900. [PubMed: 15932889]

Bernasconi N. Mesial temporal damage in temporal lobe epilepsy: a volumetric MRI study of the hippocampus, amygdala and parahippocampal region. Brain. 2003; 126:462–469. [PubMed: 12538412]

Bertram EH, Cornett JF. The evolution of a rat model of chronic spontaneous limbic seizures. Brain Res. 1994; 661:157–162. [PubMed: 7834366]

Blumenfeld H, Lampert A, Klein JP, Mission J, Chen MC, Rivera M, Dib-Hajj S, Brennan AR, Hains BC, Waxman SG. Role of hippocampal sodium channel Nav1.6 in kindling epileptogenesis. Epilepsia. 2009; 50:44–55.

Boiko T, Rasband MN, Levinson SR, Caldwell JH, Mandel G, Trimmer JS, Matthews G. Compact myelin dictates the differential targeting of two sodium channel isoforms in the same axon. Neuron. 2001; 30:91–104. [PubMed: 11343647]

Buckmaster PS, Dudek FE. Network properties of the dentate gyrus in epileptic rats with hilar neuron loss and granule cell axon reorganization. J Neurophysiol. 1997; 77:2685–2696. [PubMed: 9163384]

Cavazos JE, Jones SM, Cross DJ. Sprouting and synaptic reorganization in the subiculum and CA1 region of the hippocampus in acute and chronic models of partial-onset epilepsy. Neuroscience. 2004; 126:677–88. [PubMed: 15183517]

Cohen I, Navarro V, Clemenceau S, Baulac M, Miles R. On the origin of interictal activity in human temporal lobe epilepsy in vitro. Science (80-). 2002; 298:1418–1421.

Crill WE. Persistent sodium current in mammalian central neurons. Annu Rev Physiol. 1996; 58:349–62. [PubMed: 8815799]

Dawodu S, Thom M. Quantitative neuropathology of the entorhinal cortex region in patients with hippocampal sclerosis and temporal lobe epilepsy. Epilepsia. 2005; 46:23–30. [PubMed: 15660765]

de Guzman P, Inaba Y, Biagini G, Baldelli E, Mollinari C, Merlo D, Avoli M. Subiculum network excitability is increased in a rodent model of temporal lobe epilepsy. Hippocampus. 2006; 16:843–60. [PubMed: 16897722]

Ellerkmann RK, Remy S, Chen J, Sochivko D, Elger CE, Urban BW, Becker A, Beck H. Molecular and functional changes in voltage-dependent Na(+) channels following pilocarpine-induced status epilepticus in rat dentate granule cells. Neuroscience. 2003; 119:323–333. [PubMed: 12770549]

Fisher PD, Sperber EF, Moshé SL. Hippocampal sclerosis revisited. Brain Dev. 1998; 20:563–573. [PubMed: 9865538]

Fujita S, Toyoda I, Thamattoor AK, Buckmaster PS. Preictal activity of subicular, CA1, and dentate gyrus principal neurons in the dorsal hippocampus before spontaneous seizures in a rat model of temporal lobe epilepsy. J Neurosci. 2014; 34:16671–87. [PubMed: 25505320]

Grieco TM, Malhotra JD, Chen C, Isom LL, Raman IM. Open-channel block by the cytoplasmic tail of sodium channel beta4 as a mechanism for resurgent sodium current. Neuron. 2005; 45:233–44. [PubMed: 15664175]

Hargus NJ, Merrick EC, Nigam A, Kalmar CL, Baheti AR, Bertram EH, Patel MK. Temporal lobe epilepsy induces intrinsic alterations in Na channel gating in layer II medial entorhinal cortex neurons. Neurobiol Dis. 2011; 41:361–76. [PubMed: 20946956]

Hargus NJ, Nigam A, Bertram EH, Patel MK. Evidence for a role of Nav1.6 in facilitating increases in neuronal hyperexcitability during epileptogenesis. J Neurophysiol. 2013; 110:1144–57. [PubMed: 23741036]

Harris E, Stewart M. Propagation of synchronous epileptiform events from subiculum backward into area CA1 of rat brain slices. Brain Res. 2001; 895:41–49. [PubMed: 11259758]

Houser CR. Granule cell dispersion in the dentate gyrus of humans with temporal lobe epilepsy. Brain Res. 1990; 535:195–204. [PubMed: 1705855]

Hu W, Tian C, Li T, Yang M, Hou H, Shu Y. Distinct contributions of Na(v)1.6 and Na(v)1.2 in action potential initiation and backpropagation. Nat Neurosci. 2009; 12:996–1002. [PubMed: 19633666]

Kaplan MR, Cho MH, Ullian EM, Isom LL, Levinson SR, Barres BA. Differential control of clustering of the sodium channels Nav1.2 and Nav1.6 at developing CNS nodes of Ranvier. Neuron. 2001; 30:105–119. [PubMed: 11343648]

Ketelaars SO, Gorter JA, van Vliet EA, Lopes da Silva FH, Wadman WJ. Sodium currents in isolated rat CA1 pyramidal and dentate granule neurones in the post-status epilepticus model of epilepsy. Neuroscience. 2001; 105:109–120. [PubMed: 11483305]

Knopp A, Kivi A, Wozny C, Heinemann U, Behr J. Cellular and network properties of the subiculum in the pilocarpine model of temporal lobe epilepsy. J Comp Neurol. 2005; 483:476–88. [PubMed: 15700275]

Kwan P, Sander JW. The natural history of epilepsy: an epidemiological view. J Neurol Neurosurg Psychiatry. 2004; 75:1376–1381d. [PubMed: 15377680]

Lewis AH, Raman IM. Resurgent current of voltage-gated Na(+) channels. J Physiol. 2014; 592:4825–38. [PubMed: 25172941]

Lothman EW, Bertram EH, Bekenstein JW, Perlin JB. Self-sustaining limbic status epilepticus induced by “continuous” hippocampal stimulation: electrographic and behavioral characteristics. Epilepsy Res. 1989; 3:107–119. [PubMed: 2707248]

Makinson CD, Tanaka BS, Lamar T, Goldin AL, Escayg A. Role of the hippocampus in Nav1.6 (Scn8a) mediated seizure resistance. Neurobiol Dis. 2014; 68:16–25. [PubMed: 24704313]

Mathern GW, Babb TL, Pretorius JK, Melendez M, Levesque MF. The pathophysiologic relationships between lesion pathology, intracranial ictal EEG onsets, and hippocampal neuron losses in temporal lobe epilepsy. Epilepsy Res. 1995; 21:133–147. [PubMed: 7588588]

Mattia D, Hwa GG, Avoli M. Membrane properties of rat subicular neurons in vitro. J Neurophysiol. 1993; 70:1244–8. [PubMed: 8229171]

Naber PA, Lopes da Silva FH, Witter MP. Reciprocal connections between the entorhinal cortex and hippocampal fields CA1 and the subiculum are in register with the projections from CA1 to the subiculum. Hippocampus. 2001; 11:99–104. [PubMed: 11345131]

O’Mara SM, Commins S, Anderson M, Gigg J. The subiculum: A review of form, physiology and function. Prog Neurobiol. 2001

Patel RR, Barbosa C, Brustovetsky T, Brustovetsky N, Cummins TR. Aberrant epilepsy-associated mutant Nav1.6 sodium channel activity can be targeted with cannabidiol. Brain. 2016; 139:2164–81. [PubMed: 27267376]

Patino GA, Isom LL. Electrophysiology and beyond: multiple roles of Na+ channel β subunits in development and disease. Neurosci Lett. 2010; 486:53–9. [PubMed: 20600605]

Paxinos G, Watson C. The Rat Brain in Stereotaxic Coordinates Sixth Edition by. Acad Press. 2006; 170:547612.

Petersen AV, Jensen CS, Crépel V, Falkerslev M, Perrier J-F. Serotonin Regulates the Firing of Principal Cells of the Subiculum by Inhibiting a T-type Ca2+ Current. Front Cell Neurosci. 2017:11. [PubMed: 28217083]

Raman IM, Bean BP. Resurgent sodium current and action potential formation in dissociated cerebellar Purkinje neurons. J Neurosci. 1997; 17:4517–26. [PubMed: 9169512]

Rosker C, Lohberger B, Hofer D, Steinecker B, Quasthoff S, Schreibmayer W. The TTX metabolite 4,9-anhydro-TTX is a highly specific blocker of the Na(v1.6) voltage-dependent sodium channel. Am J Physiol Cell Physiol. 2007; 293:C783–C789. [PubMed: 17522141]

Royeck M, Horstmann MT, Remy S, Reitze M, Yaari Y, Beck H. Role of axonal NaV1.6 sodium channels in action potential initiation of CA1 pyramidal neurons. J Neurophysiol. 2008; 100:2361–80. [PubMed: 18650312]

Rush AM, Dib-Hajj SD, Waxman SG. Electrophysiological properties of two axonal sodium channels, Nav1.2 and Nav1.6, expressed in mouse spinal sensory neurones. J Physiol. 2005; 564:803–15. [PubMed: 15760941]

Sanabria ERG, Su H, Yaari Y. Initiation of network bursts by Ca 2 +-dependent intrinsic bursting in the rat pilocarpine model of temporal lobe epilepsy. J Physiol. 2001; 532:205–216. [PubMed: 11283235]

Shao LR, Dudek FE. Electrophysiological evidence using focal flash photolysis of caged glutamate that CA1 pyramidal cells receive excitatory synaptic input from the subiculum. J Neurophysiol. 2005; 93:3007–3011. [PubMed: 15601737]

Spencer SS, Spencer DD. Entorhinal-hippocampal interactions in medial temporal lobe epilepsy. Epilepsia. 1994; 35:721–7. [PubMed: 8082614]

Staff NP, Jung HY, Thiagarajan T, Yao M, Spruston N. Resting and active properties of pyramidal neurons in subiculum and CA1 of rat hippocampus. J Neurophysiol. 2000; 84:2398–408. [PubMed: 11067982]

Stafstrom CE. Persistent Sodium Current and Its Role in Epilepsy. Epilepsy Curr. 2007; 7:15–22. [PubMed: 17304346]

Stafstrom CE. Epilepsy and Epileptogenesis. Epilepsy Curr. 2005; 5:121–129. [PubMed: 16151518]

Stewart M, Wong RK. Intrinsic properties and evoked responses of guinea pig subicular neurons in vitro. J Neurophysiol. 1993; 70:232–45. [PubMed: 8395577]

Swanson LW, Cowan WM. An autoradiographic study of the organization of the efferent connections of the hippocampal formation in the rat. J Comp Neurol. 1977; 172:49–84. [PubMed: 65364]

Tang H, Wu GS, Xie J, He X, Deng K, Wang H, Xu F, Luo HR. Brain-wide map of projections from mice ventral subiculum. Neurosci Lett. 2016; 629:171–179. [PubMed: 27422730]

Taube J. Electrophysiological properties of neurons in the rat subiculum in vivo. Exp Brain Res. 1993; 96:304–318. [PubMed: 7903643]

Toyoda I, Bower MR, Leyva F, Buckmaster PS. Early activation of ventral hippocampus and subiculum during spontaneous seizures in a rat model of temporal lobe epilepsy. J Neurosci. 2013; 33:11100–15. [PubMed: 23825415]

van Drongelen W, Koch H, Elsen FP, Lee HC, Mrejeru A, Doren E, Marcuccilli CJ, Hereld M, Stevens RL, Ramirez JM. Role of persistent sodium current in bursting activity of mouse neocortical networks in vitro. J Neurophysiol. 2006; 96:2564–77. [PubMed: 16870839]

Van Wart A, Matthews G. Impaired firing and cell-specific compensation in neurons lacking nav1.6 sodium channels. J Neurosci. 2006; 26:7172–7180. [PubMed: 16822974]

Veeramah KR, O'Brien JE, Meisler MH, Cheng X, Dib-Hajj SD, Waxman SG, Talwar D, Girirajan S, Eichler EE, Restifo LL, Erickson RP, Hammer MF. De novo pathogenic SCN8A mutation identified by whole-genome sequencing of a family quartet affected by infantile epileptic encephalopathy and SUDEP. Am J Hum Genet. 2012; 90:502–510. [PubMed: 22365152]

Vreugdenhil M, Hoogland G, van Veelen CW, Wadman WJ. Persistent sodium current in subicular neurons isolated from patients with temporal lobe epilepsy. Eur J Neurosci. 2004; 19:2769–2778. [PubMed: 15147310]

Wagnon JL, Korn MJ, Parent R, Tarpey TA, Jones JM, Hammer MF, Murphy GG, Parent JM, Meisler MH. Convulsive seizures and SUDEP in a mouse model of SCN8A epileptic encephalopathy. Hum Mol Genet. 2015; 24:506–15. [PubMed: 25227913]

Wellmer J, Su H, Beck H, Yaari Y. Long-lasting modification of intrinsic discharge properties in subicular neurons following status epilepticus. Eur J Neurosci. 2002; 16:259–266. [PubMed: 12169108]

Whitaker WRJ, Faull RLM, Dragunow M, Mee EW, Emson PC, Clare JJ. Changes in the mRNAs encoding voltage-gated sodium channel types II and III in human epileptic hippocampus. Neuroscience. 2001; 106:275–285. [PubMed: 11566500]

Witter MP, Groenewegen HJ. The subiculum: cytoarchitectonically a simple structure, but hodologically complex. Prog Brain Res. 1990; 83:47–58. [PubMed: 2392570]

Witter MP, Naber PA, Van Haeften T, Machielsen WCM, Rombouts SARB, Barkhof F, Scheltens P, Lopes Da Silva FH. Cortico-hippocampal communication by way of parallel parahippocampal-subicular pathways. Hippocampus. 2000; 10:398–410. [PubMed: 10985279]

Witter MP, Wouterlood FG, Naber PA, Van Haeften T. Anatomical organization of the parahippocampal-hippocampal network. Ann N Y Acad Sci. 2000; 911:1–24. [PubMed: 10911864]

Wozny C, Knopp A, Lehmann TN, Heinemann U, Behr J. The subiculum: a potential site of ictogenesis in human temporal lobe epilepsy. Epilepsia. 2005; 46(Suppl 5):17–21.

Yue C, Remy S, Su H, Beck H, Yaari Y. Proximal persistent Na+ channels drive spike after depolarizations and associated bursting in adult CA1 pyramidal cells. J Neurosci. 2005; 25:9704–9720. [PubMed: 16237175]

Highlights

- In a rat model of temporal lobe epilepsy (TLE), subiculum neurons are hyperexcitable.
- TLE subiculum neurons show pro-excitatory alterations in sodium channel physiology.
- Increased resurgent and persistent sodium currents are seen in the subiculum in TLE.
- Inhibiting $Na_V1.6$ attenuates neuronal hyperxcitability in the subiculum in TLE.

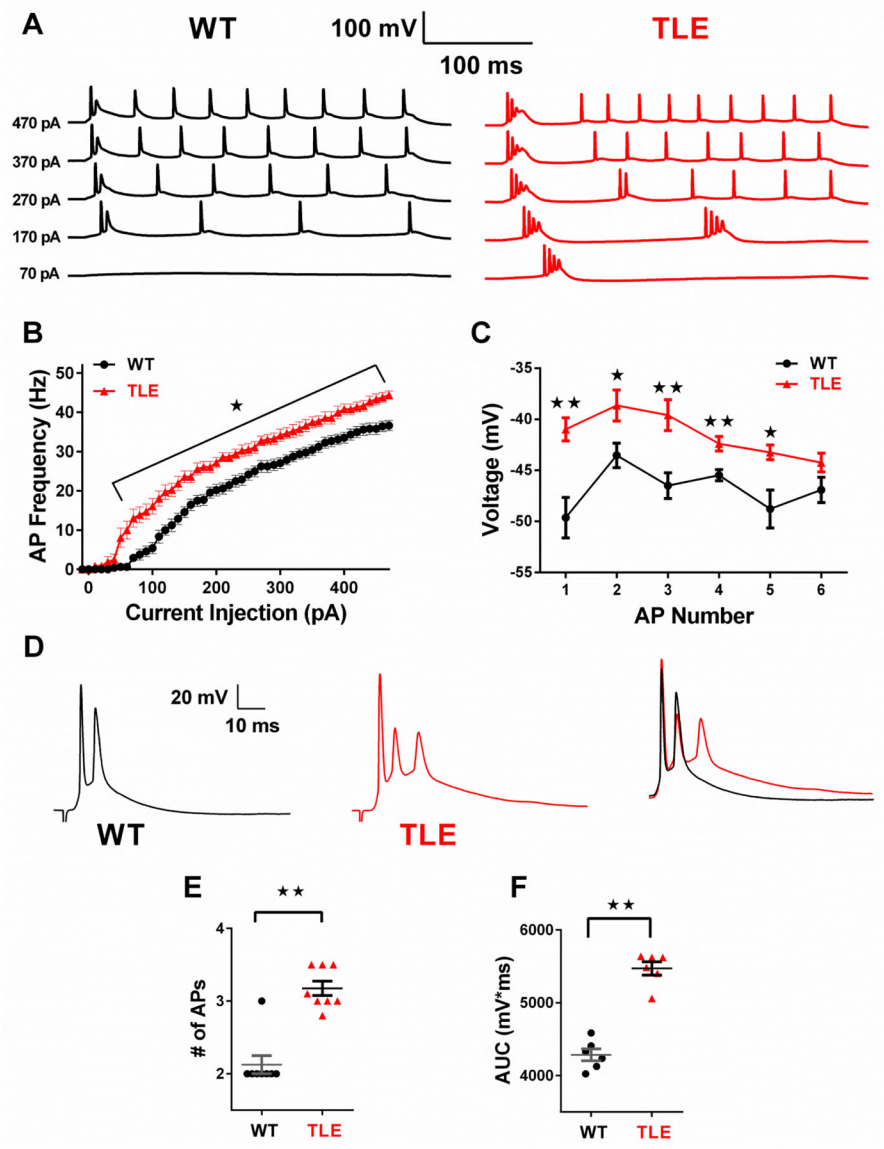

Figure 1. Subiculum neurons are hyperexcitable in TLE

(A) Representative traces of APs elicited by 300 ms current injection steps of increasing amplitude from a holding potential of −65 mV. (B) AP frequency versus injected current plot shows higher neuronal firing frequency in TLE (n=12) neurons compared to control (n=16). (C) Plot of maximal hyperpolarizing voltages reached between APs evoked by a 270 pA depolarizing current injection step. (D) Brief stimulation of the CA1 pyramidal layer elicited synaptically evoked AP bursts in WT (n=8) and TLE neurons (n=8). Right; superimposed traces of WT, black and TLE, red synaptically evoked responses shows increased response duration and spiking in TLE subiculum neurons compared with WT. (E) Scatter plot showing AP spiking frequency in response to synaptic stimulation. (F) Scatter plot showing area under the curve (AUC) for synaptically evoked APs. Data represent mean ± S.E.M. Statistical significance: *P<0.05; **P<0.01 Student's T-Test with Welch's correction.

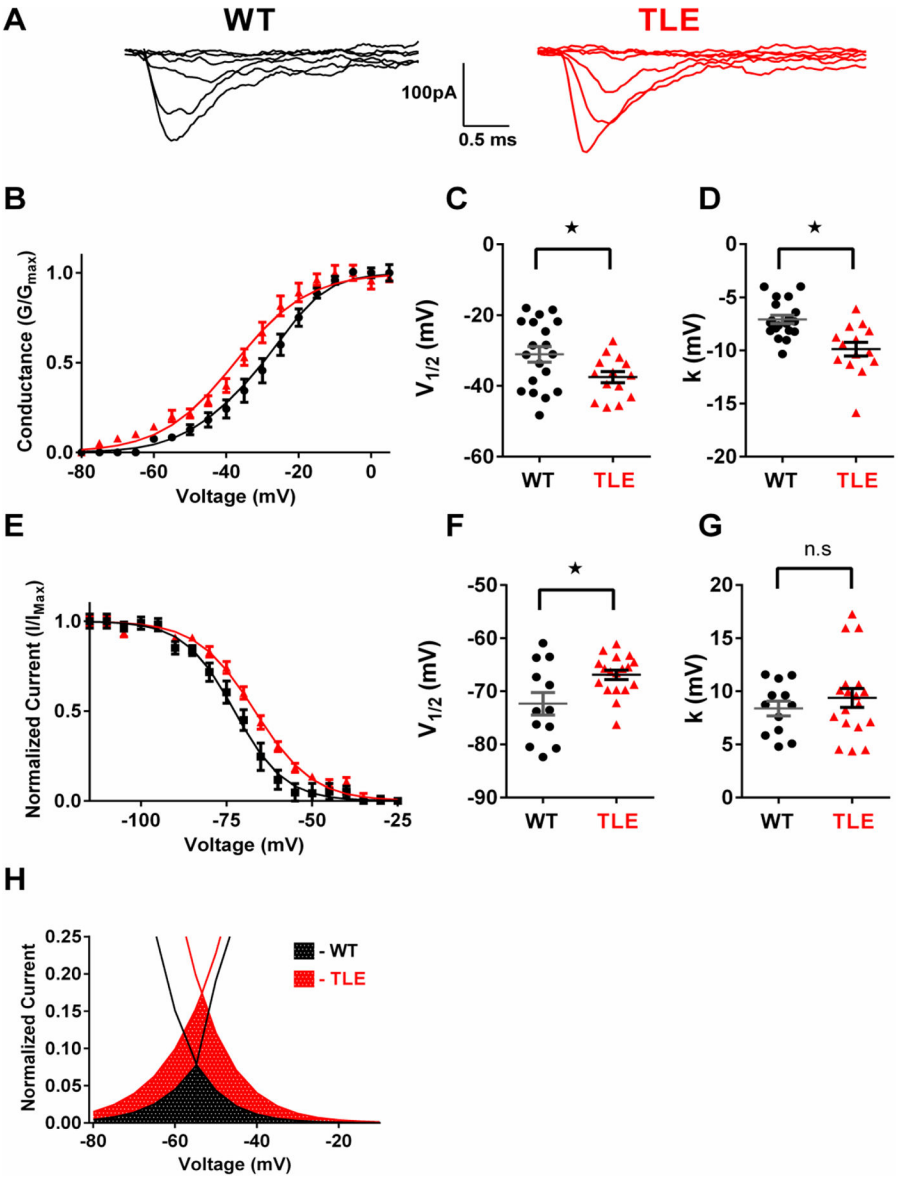

Figure 2. TLE subiculum neurons exhibit pro-excitatory alterations in sodium channel physiology

(A) Representative current traces recorded using the outside-out patch clamp configuration for WT and TLE subiculum neurons. (B) Voltage dependence of channel activation for WT (black, n=19) and TLE (red, n=14) subiculum neurons. Lines correspond to the least-squares fit when average data were fit to a single Boltzmann equation. (C) Scatter plot of voltage at half-maximal activation ($V_{1/2}$) for WT and TLE subiculum neurons. (D) Scatter plot of the slope factor (k) of activation in WT and TLE subiculum neurons. (E) Voltage dependence of channel inactivation for WT (black, n=12) and TLE (red, n=18) subiculum neurons. Lines correspond to the least-squares fit when average data were fit to a single Boltzmann equation. (F) Scatter plot of voltage at half-maximal inactivation ($V_{1/2}$) for WT and TLE subiculum neurons. (G) Scatter plot of the slope factor (k) of inactivation. (H) Window current predicted by overlapping normalized activation and inactivation curves. Estimated

window current is elevated in TLE subiculum neurons (red checkered area) compared to WT (black checkered area). Data represent mean ± S.E.M. Statistical significance: *P<0.05 Student's T-Test with Welch's correction.

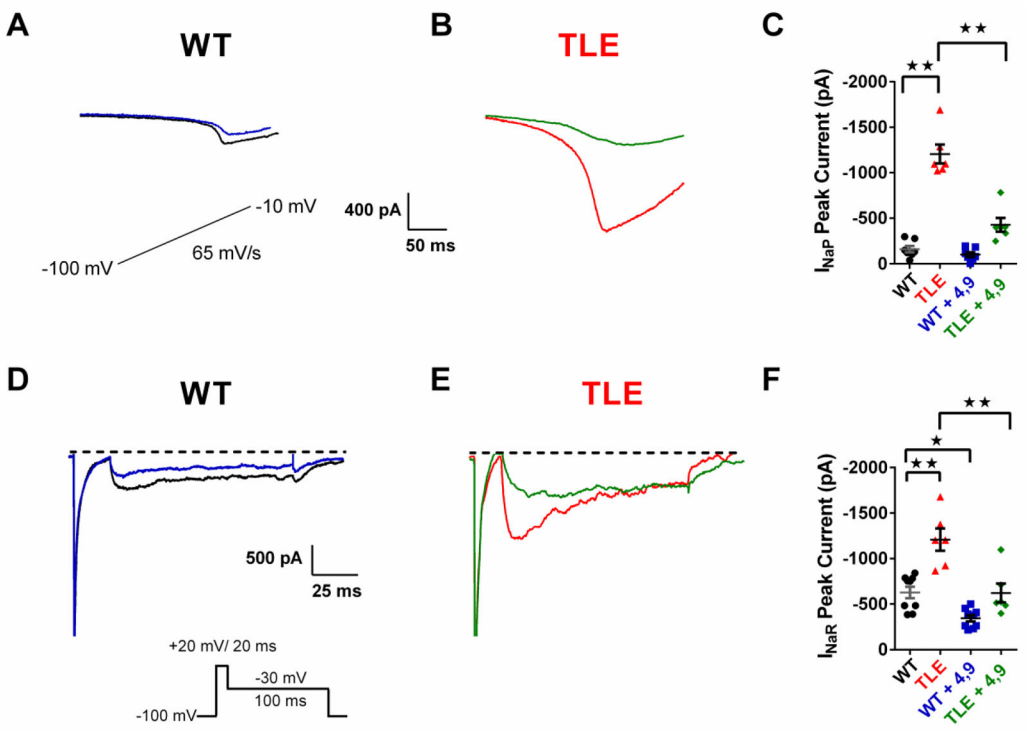

Figure 3. TLE subiculum neurons show increased persistent (I_{NaP}) and resurgent (I_{NaR}) sodium currents that are attenuated by 4,9-anhydro-tetrodotoxin

I_{NaP} currents were elicited by applying a voltage ramp at a rate of 65 mV/s (inset of A). Recordings were repeated in the presence of TTX (1 μM). Traces shown are those obtained after subtracting traces recorded in the presence of TTX. (A) I_{NaP} currents in WT subiculum neurons are reduced by 4,9-ah-TTX (100 nM: WT, black; WT + 4,9-ah-TTX, blue). (B) I_{NaP} currents in TLE subiculum neurons are increased compared with WT and significantly attenuated by 4,9-ah-TTX (100 nM: TLE, red; TLE + 4,9-ah-TTX, green). (C) Scatter plot of I_{NaP} peak amplitudes pre and post application of 4,9-ah-TTX in WT and TLE subiculum neurons (WT, black, n=7; TLE, red, n=6; WT + 4,9-ah-TTX, blue, n=7; TLE + 4,9-ah-TTX, green, n=6). I_{NaR} currents recorded from subiculum neurons using the voltage protocols shown. Traces shown were obtained after subtraction of recordings obtained in the presence of TTX (1 μM). (D) I_{NaR} currents in WT neurons were reduced by 4,9-ah-TTX (100 nM: WT, black; WT + 4,9-ah-TTX, blue). (E) I_{NaR} currents in TLE neurons were larger than those recorded in WT neurons and significantly attenuated by 4,9-ah-TTX (100 nM: TLE, red, TLE + 4,9-ah-TTX (100 nM), green). (F) Scatter plot of I_{NaR} peak amplitudes before and after bath application of 4,9-ah-TTX (100 nM) for WT (WT, black, n=9; WT + 4,9-ah-TTX (100 nM), blue, n=9) and TLE neurons (TLE, red, n=6; TLE + 4,9-ah-TTX (100 nM), green, n=6). Data represent mean ± S.E.M. Statistical significance: *p<0.05; **p<0.01 Student's T-Test with Welch's correction.

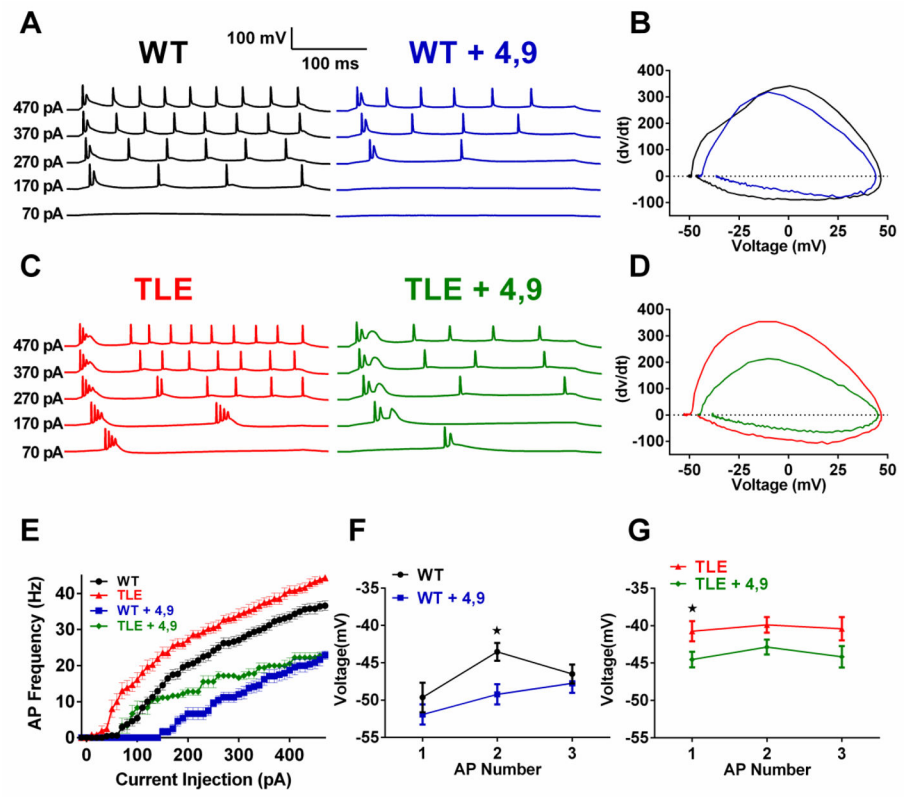

Figure 4. Inhibition of $Na_V1.6$ currents by 4,9-ah-TTX decreases neuronal excitability in subiculum bursting neurons

(A) Representative traces of APs elicited by 300 ms current injection steps of increasing current amplitude in WT (A) (WT, black, WT + 4,9-ah-TTX (100 nM), blue) (B) Representative phase plot analysis of the first elicited AP in WT neurons before and after the application of 4,9-ah-TTX (WT, black; WT + 4,9-ah-TTX (100 nM), blue) (C) Representative traces of APs elicited by 300 ms current injection steps of increasing current amplitude in TLE neurons (TLE, red; TLE + 4,9-ah-TTX (100 nM), green) (D) Representative phase plot analysis of the first elicited AP in TLE neurons before and after the application of 4,9-ah-TTX (TLE, red; TLE + 4,9 ah-TTX (100 nM), green). (E) Effects of 4,9-ah-TTX (100 nM) on AP frequency for WT and TLE subiculum neurons (WT, black, n=16; WT + 4,9-ah-TTX, blue, n=7; TLE, red, n=12; TLE + 4,9-ah-TTX, green, n=6). Effects of 4,9-ah-TTX (100 nM) on maximal hyperpolarizing voltages between the first 3 APs evoked by a 270 pA current injection in WT (F) and TLE subiculum neurons (G). Data represent mean ± S.E.M. Statistical significance: *P<0.05 Student's T-Test with Welch's correction.

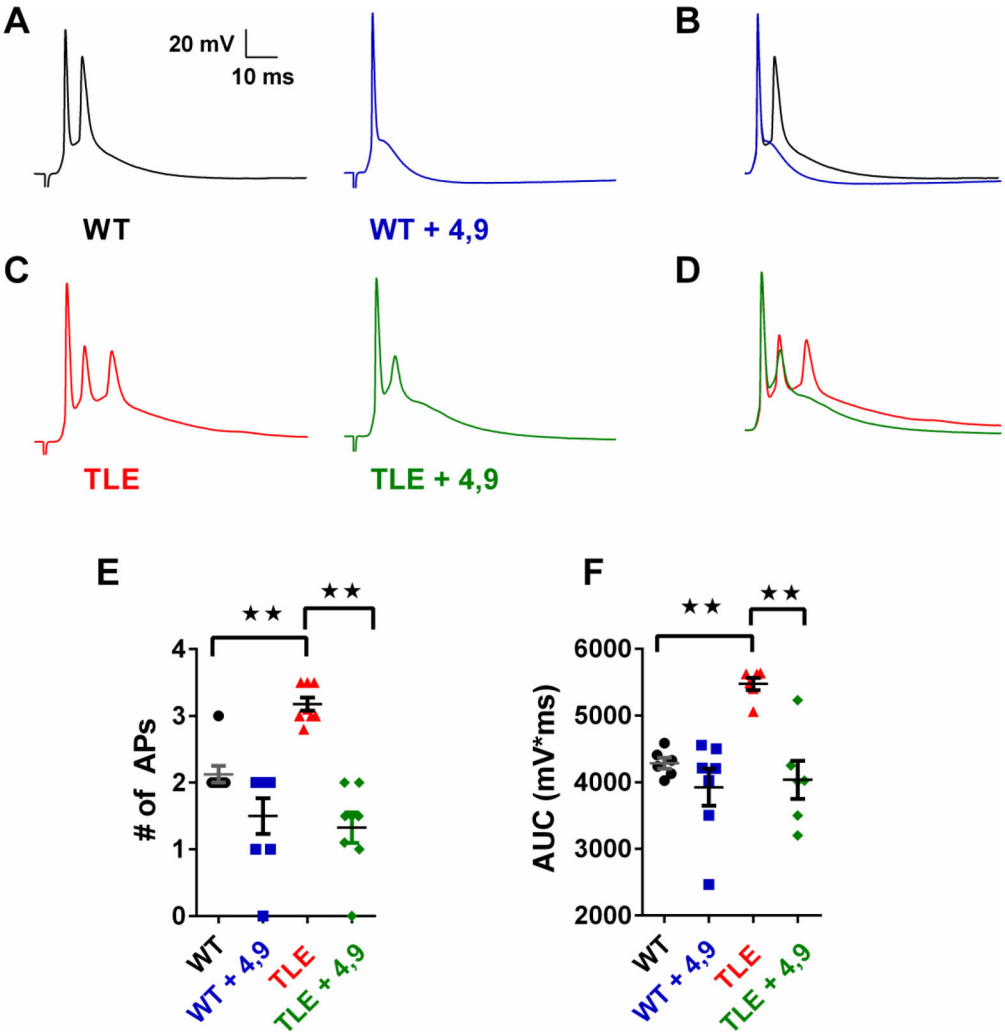

Figure 5. Inhibition of $Na_V1.6$ currents by 4,9-ah-TTX attenuates synaptically evoked burst firing in TLE subiculum neurons

(A) Application of 4,9-ah-TTX (100 nM) reduces synaptically evoked AP bursts in WT and (C) TLE subiculum neurons. Superimposed traces for WT (B) and TLE (D) subiculum neurons illustrate effects of 4,9 ah-TTX (100 nM) on evoked responses. (E) Scatter plot showing AP frequency in response to synaptic stimulation before and after application of 4,9-ah-TTX (100 nM: WT, black, n=8; WT + 4,9-ah-TTX, blue, n=8; TLE, red, n=8; TLE + 4,9-ah-TTX; green, n=8). (F) Scatter plot showing area under the curve (AUC) for synaptically evoked APs. Data represent mean ± S.E.M. Statistical significance: **P<0.01 Student's T-Test with Welch's correction.

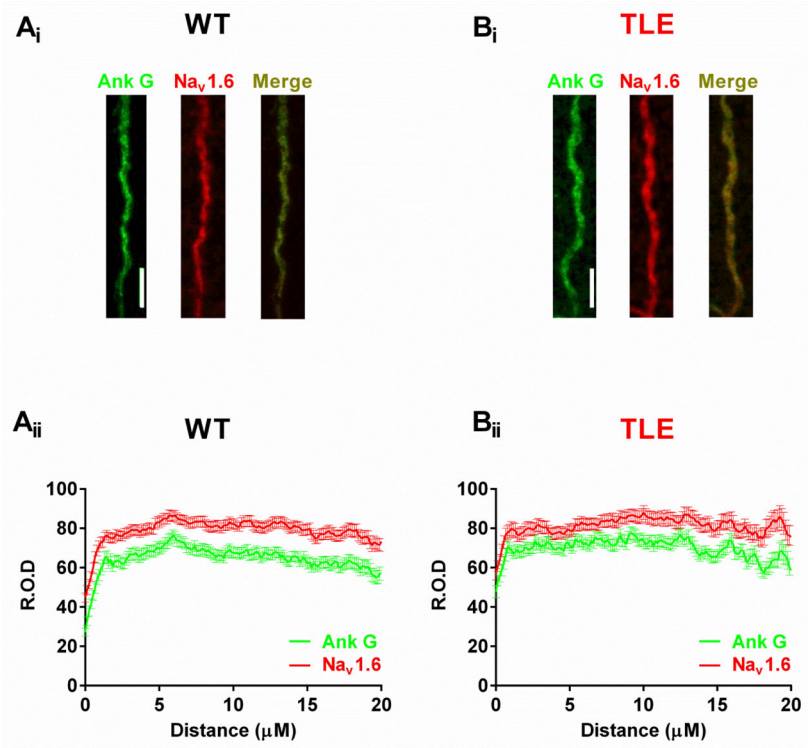

Figure 6. $Na_v1.6$ AIS staining is not increased in TLE subiculum neurons compared to WT

Na_v 1.6 staining along the AIS of WT (A_i) and TLE (B_i) subiculum neurons (Ank G, green; $Na_v1.6$, red; Merge; yellow). Graphs showing the localization and relative optical density (R.O.D) of Ank G and $Na_v1.6$ staining along the length of the AIS for WT (A_{ii}) and TLE (B_{ii}) subiculum neurons (WT, n=191 AIS from 4 animals; TLE, n=140 AIS from 4 animals). Scale bars represent 5 μm. Data represent mean ± S.E.M.

Table 1

Membrane Properties of WT and TLE Subiculum Neurons

	RMP, mV	R_i, MΩ	Threshold, mV	Amplitude, mV	AP Width (ms)	Upstroke Velocity, mV/ms	Rheobase (pA)	N
WT	−61.3 ± 0.2	66.0 ± 2.9	−45.7 ± 0.3	96.6 ± 0.8	0.87 ± 0.0	359.0 ± 18.5	94.4 ± 5.0	16
TLE	−61.5 ± 0.2	86.8 ± 5.1 **	−50.4 ± 0.6 **	98.9 ± 1.4	0.95 ± 0.0 **	315.8 ± 27.2	50.8 ± 5.3 **	12
WT + 4,9-ah-TTX (100 nM)	−59.3 ± 0.3 ††	48.9 ± 2.7 ††	−41.6 ± 0.3 ††	90.0 ± 1.6 ††	0.99 ± 0.0 ††	346.2 ± 16.0	188 ± 10.8 ††	7
TLE + 4,9-ah-TTX (100 nM)	−59.6 ± 0.2 ††	76.8 ± 9.7	−42.9 ± 0.4 ††	95.0 ± 2.9	1.1 ± 0.3 ††	243.1 ± 20.3 †	100 ± 7.3 ††	6

Values represent mean ± S.E.M, n= number of cells. RMP; Resting membrane potential. R_i; input resistance.

** p<0.01 compared to WT,

† p<0.05 compared to no 4,9-ah-TTX,

†† p<0.01 compared to no 4,9-ah-TTX, Student's T-test with Welch's Correction

Table 2

Sodium Channel Physiology in WT and TLE Subiculum Neurons

	Activation			Inactivation		
	$V_{1/2}$ (mV)	**k (mV)**	**n**	**$V_{1/2}$ (mV)**	**k (mV)**	**n**
WT	−31.3 ± 2.2	−7.1 ± 0.4	19	−72.6 ± 2.1	8.4 ± 0.7	12
TLE	−37.5 ± 1.6*	−9.9 ± 0.6*	14	−66.9 ± 0.9*	9.4 ± 0.9	18

Values represent mean ± S.E.M, n= number of cells. $V_{½}$, voltage of half-maximal activation or inactivation; k, slope factor.

*P<0.05 vs WT, Student's T-test with Welch's Correction